

Meson and Quark Degrees of Freedom and the Radius of the Deuteron

A. J. Buchmann*, H. Henning, and P. U. Sauer

Institute for Theoretical Physics

University of Hannover

Appelstraße 2

D-30167 Hannover

Germany

August 14, 2018

Abstract

The existing experimental data for the deuteron charge radius are discussed. The data of elastic electron scattering are inconsistent with the value obtained in a recent atomic physics experiment. Theoretical predictions based on a nonrelativistic description of the deuteron with realistic nucleon-nucleon potentials and with a rather complete set of meson-exchange contributions to the charge operator are presented. Corrections arising from the quark-gluon substructure of the nucleon are explored in a nonrelativistic quark model; the quark-gluon corrections, not accounted for by meson exchange, are small. Our prediction for the deuteron charge radius favors the value of a recent atomic physics experiment.

PACS number(s): 21.45.+v, 21.10.Ft, 25.30.Bf, 27.10+h, 12.39.Pn

1. Introduction

Deuteron properties are quantities of fundamental importance. The hadronic properties are used to calibrate parametrizations of the nucleon-nucleon (NN) interaction. The electromagnetic (e.m.) properties are crucial tests of the theory of e.m. currents, but simultaneously also of the chosen form of the NN interaction. Although there has been a continuous interest in all deuteron observables, the observable root-mean-square (rms) charge radius r_{ch} and the related but unobservable rms matter radius r_m have recently received special attention [1, 4, 2, 3, 5, 6, 7, 8]. This is mainly due to unresolved discrepancies between experimental data and theoretical predictions. These discrepancies have even led to speculations [3, 7, 8] that quark-gluon effects may surface in the deuteron charge radius. We are sceptical that these effects can resolve the observed discrepancies. Nevertheless, possible quark-gluon effects in the deuteron charge radius deserve a careful investigation. This is the reason why this paper studies general short-range corrections of hadronic and of quark-gluon nature for the deuteron charge radius, not discussed before. With respect to the history of the subject,

*Present Address: Institute of Theoretical Physics, University of Tübingen, Auf der Morgenstelle 14, D-72076 Tübingen, Germany

Ref. [9] gives a comprehensive review of both experimental and theoretical aspects of the deuteron radius.

Sect. 2 summarizes the existing experimental data of elastic electron scattering and of an atomic physics experiment relevant for the deuteron charge radius. It does not contain novel material. Despite the review of Ref. [9] the section is important for this paper, since it sets the stage for our calculations; it extends our discussion in Ref. [10]. All calculations of deuteron charge properties require meson-exchange (MEC) corrections for the charge operator. Sect. 3 presents our theoretical predictions. Subsect. 3.1 discusses them in a hadronic description of the deuteron. Subsect. 3.2 extends this description by taking the quark-gluon substructure of nucleons into account. We give our conclusions on the unresolved discrepancy between experimental data and theoretical predictions in Sect. 4.

2. Experimental Data and their Analyses

The mean square (ms) deuteron charge radius r_{ch}^2 is defined as the slope of the deuteron charge monopole form factor $F_{ch}(\mathbf{Q}^2)$ of elastic electron scattering at zero three-momentum transfer \mathbf{Q} , i.e.,

$$r_{ch}^2 = -6 \frac{d}{d\mathbf{Q}^2} F_{ch}(\mathbf{Q}^2) |_{\mathbf{Q}^2=0}. \quad (1)$$

Equivalently, it can be derived from the slope of the deuteron longitudinal structure function $A(\mathbf{Q}^2)$ at zero momentum transfer, corrected for a small contribution arising from the deuteron magnetic moment μ_d measured in units of nuclear magnetons $\mu_N = e/2M_p$, where M_p is the proton mass,

$$r_{ch}^2 = -3 \frac{d}{d\mathbf{Q}^2} A(\mathbf{Q}^2) |_{\mathbf{Q}^2=0} + \frac{\mu_d^2}{2M_p^2}. \quad (2)$$

The latter correction $\mu_d^2/2M_p^2 = 0.0163 \text{ fm}^2$ arises, since the longitudinal structure function $A(\mathbf{Q}^2)$ is built up from the charge monopole, charge quadrupole and magnetic dipole form factors $F_{ch}(\mathbf{Q}^2)$, $F_q(\mathbf{Q}^2)$ and $F_m(\mathbf{Q}^2)$ according to $A(\mathbf{Q}^2) = F_{ch}^2(\mathbf{Q}^2) + \mathbf{Q}^4/18 F_q^2(\mathbf{Q}^2) + \mathbf{Q}^2/6M_p^2 F_m^2(\mathbf{Q}^2)$ [11]; the form factors are considered in the Breit frame in which $\mathbf{Q}^2 = -q^2$, q being the four-momentum transfer. The charge quadrupole and the magnetic dipole form factors are normalized to the deuteron quadrupole moment in units of fm^2 and to the deuteron magnetic moment in units of μ_N , respectively.

Characteristic experimental data for $A(\mathbf{Q}^2)$ at small momentum transfers are displayed in Fig. 1(a). They are obtained in elastic electron scattering; the bearing of the experimental charge radius, measured by the isotope shift of the $1s - 2s$ transition of atomic hydrogen, on $A(\mathbf{Q}^2)$ is displayed in Fig. 1(b). In Fig. 1, we use the standard form of a high-resolution plot which emphasizes experimental errors and possible inconsistencies between experiments. We see that $A(\mathbf{Q}^2)$ is at low momentum transfers not determined with the desired accuracy. Furthermore, the data of Refs. [12] and [13] show opposing trends as already emphasized in Ref. [13]; however, the low-momentum transfer data of Ref. [12] have always been considered reliable beyond any doubt, whereas those of Ref. [13] have set a new standard of experimental accuracy at intermediate momentum transfers. Thus, the discrepancies between both data sets create general worries about the low-momentum transfer data, most important for extracting the deuteron charge radius r_{ch} .

Elastic electron scattering is often simultaneously performed on deuteron and proton targets. The advantage of such a simultaneous measurement is that the corresponding ratio of deuteron and proton charge form factors, $F_{ch}(\mathbf{Q}^2)/G_{Ep}(\mathbf{Q}^2)$, can be extracted with a

Experiment	r_{ch} [fm]	r_d [fm]	r_p [fm]	r_n^2 [fm ²]	r_{ch} [fm]
Berard <i>et al.</i> [15]	2.1256(64)	1.9635(45)	0.805(11)	-0.1134(24)	2.0952(60)
Akimov <i>et al.</i> [16]	2.098 (26)	1.935 (28)	0.817(8)	-0.1170(18)	2.080 (27)
Simon <i>et al.</i> [12] ^a	2.1159(65)	1.9540(47)	0.862(12)	-0.1170(18)	2.1160(60)
Simon <i>et al.</i> [12] ^b	2.1193(80)	1.9576(68)	0.862(12)	-0.1170(18)	2.1190(80)
Schmidt-Kaler <i>et al.</i> [14]	2.1303(66)	1.9685(49)	0.862(12)	-0.1130(30)	2.1303(66)

Table 1: **Experimental structure radius r_d and charge radius r_{ch} of the deuteron.**

Results are given for three elastic electron scattering experiments [12, 15, 16], and for an atomic physics experiment [14]. The *experimental* values [12, 15, 16] for the structure radius r_d as defined in Eq. (3) are listed in column 2; the *resulting* deuteron charge radii using the proton and neutron charge radii employed in these references are given in columns 3 to 5. In column 1 we derive updated values for the deuteron charge radius r_{ch} starting from the experimental structure radius r_d of column 2. For this purpose we use the presently accepted value for the proton charge radius, i.e., $r_p = 0.862(12)$ fm [17] but use the same neutron charge radius and the standard Darwin-Foldy term, $r_{DF}^2 = 0.0331$ fm², as in the respective references [12, 15, 16]. Two analyses of the data of Ref. [12] using ^(a) 3rd and ^(b) 4th order polynomials to fit the ratio $F_{ch}(\mathbf{Q}^2)/G_{Ep}(\mathbf{Q}^2)$ are quoted. The atomic physics experiment [14] gives the radius difference $(r_{ch}^2 - r_p^2)_{exp} = 3.795(19)$ fm²; the corresponding values for the charge and structure radii are obtained from Eq. (3) by using $r_p = 0.862(12)$ fm [17], $r_n^2 = -0.113(3)$ fm² [18] and $r_{DF}^2 = 0.0331$ fm².

smaller systematic error. Thus, the difference $r_{ch}^2 - r_p^2$, r_p^2 being the ms proton charge radius, is experimentally determined with higher accuracy than the deuteron charge radius itself. This is the reason why experimentalists prefer to analyze their data for the rms deuteron *structure* radius r_d , defined by

$$r_d^2 = (r_{ch}^2 - r_p^2) - r_n^2 - r_{DF}^2. \quad (3)$$

The ms structure radius contains as dominant part the experimentally determined difference $r_{ch}^2 - r_p^2$. From this one removes (i) the contribution of the neutron finite e.m. size, r_n^2 being the neutron ms charge radius, and (ii) the relativistic Darwin-Foldy correction to the nonrelativistic one-nucleon charge operator, $r_{DF}^2 = G_E^S(0)3/(4M_N^2) = 3/(4M_N^2) = 0.0331$ fm², where $G_E^S(\mathbf{Q}^2)$ is the isoscalar charge Sachs form factor of the nucleon and M_N the isospin-averaged nucleon mass. In Eq. (3), r_{ch}^2 , r_p^2 and r_n^2 are observables and r_{DF}^2 is a well-defined number. The rms deuteron structure radius r_d can therefore be considered an honest observable quantity of the same standing as the deuteron charge radius r_{ch} itself; in many experiments it is determined with even higher accuracy.

The existing experimental values for r_d and r_{ch} are listed in Table 1. The quoted values refer to the elastic electron scattering experiments of Refs. [12, 15, 16]; the experiment of Ref. [13] whose data are also shown in Fig. 1 was meant to provide information on $A(\mathbf{Q}^2)$ at intermediate momentum transfers; the authors did not extract the charge radius. The most recent experimental result on the deuteron charge radius has been obtained in an atomic isotope shift measurement [14] and is also given in Table 1. We base the discussion of the paper on the results for r_{ch} in column 1 of Table 1. We call these results experimental, although they cannot be found in the quoted references. The values quoted there are listed in columns 2 to 5. We consider the structure radius r_d in column 2 experimentally well-determined. However, in Refs. [15] and [16] the corresponding deuteron charge radii r_{ch} ,

quoted in column 5, were obtained from Eq. (3) using the proton charge radius available at that time. We therefore update the charge radius r_{ch} by using in Eq. (3) the currently accepted proton charge radius [17], i.e., $r_p = 0.862(12)$ fm, and the values r_n and r_{DF} as employed in Refs. [12, 15, 16]. We note an unsatisfactory spread of results in column 1 arising from the analyses of the considered experiments.

In addition to the charge and structure radii, theoretical papers often discuss the deuteron *matter* radius r_m ,

$$r_m^2 = \frac{1}{4} \int_0^\infty dr r^2 [u^2(r) + w^2(r)]. \quad (4)$$

It is defined in terms of the deuteron S - and D -state wave functions, i.e., $u(r)$ and $w(r)$ respectively. In Eq. (4) r stands for the relative distance between the two nucleons; a factor r^2 from the volume element is already included in the wave functions. The matter radius r_m is theoretically important because it shows the differences between deuteron wave functions, obtained from different potential models for the NN interaction, in a direct and pure, though integral form. The matter radius is conceptually interesting in the following respects:

- Due to the factor r^2 in Eq. (4) the matter radius weighs heavily the long-range part of the deuteron wave function which is dominated by one-pion exchange. All realistic parametrizations of the NN interaction have one-pion exchange tails. The corresponding matter radii typically show a spread of their values which is smaller than 1% as demonstrated later on.
- All realistic parametrizations of the NN interaction account for the deuteron binding energy with high precision. Their account of the proton-neutron spin-triplet scattering length a_t and of the asymptotic S -wave normalization A_S is far less precise. However, one observes [1, 2, 3] that the variations of a_t and A_S are linearly related to those of the matter radius r_m . At the experimental value of the scattering length $a_t = 5.419(7)$ fm according to Ref. [1, 19] the matter radius becomes $r_m = 1.969(4)$ fm. In contrast, the experimental values for the asymptotic normalization A_S [19] are not as precise as those for the triplet scattering length a_t and are even in conflict with each other. Nevertheless, they also suggest a matter radius consistent with $r_m = 1.969$ fm, though with much larger error bars [1]. Conversely, assuming the empirical correlations between a_t , A_S , and the matter radius r_m are physically reliable, the experimental value for the scattering length a_t suggests –through the intermediary of the matter radius– an asymptotic S -wave normalization $A_S = 0.885(2)$ fm^{-1/2}.

Though we prefer to discuss the model-independent deuteron charge radius r_{ch} , we admit in all fairness that the deuteron matter radius r_m is conceptually important and that it may, with the help of the well-established empirical linear relations, even serve as a measure of consistency in experimental data and in theoretical predictions for characteristic deuteron observables. Those observations are the reason why others would like to extract the deuteron matter radius also from the experimental electron scattering data. This is clearly impossible in a model-independent way, although it has been attempted often. The results of these attempts are given in Table 2.

The difference between the model-dependent ms matter radius r_m^2 and the model-independent ms charge and structure radii, r_{ch}^2 and r_d^2 , i.e.,

$$r_{ch}^2 = r_m^2 + r_p^2 + r_n^2 + r_{DF}^2 + r_{SO}^2 + r_{[2]}^2, \quad (5)$$

Analysis	r_{ch} [fm]	r_m [fm]	$r_{[2]}^2$ [fm ²]
Allen et al. [20]	2.1095(218)	1.948 (23)	0.0000
McTavish [21]	2.1204(67)	1.956 (5)	0.0150
Klarsfeld et al. [1]	2.1146(56)	1.950 (3)	0.0135
Mustafa [22]	2.1189(52)	1.9547(19)	0.0135
Wong [9]	2.1150(52)	1.9502(20)	0.0143
Schmidt-Kaler et al. [14]	2.1303(66)	1.9636(49)	0.0208
Pachucki et al. [23]	2.1331(78)	1.9666(66)	0.0208

Table 2: **Experimental charge radius r_{ch} and matter radius r_m of the deuteron.** The first five entries in column 2 are the results of various analyses [1, 9, 20, 21, 22] of elastic electron scattering data [12, 15] aiming at the matter radius r_m . The non-nucleonic correction $r_{[2]}^2$ used in these analyses is based on π -meson exchange *only*; it is listed in column 3. Our reconstruction of the charge radius is done according to Eq. (5) and given in column 1. To calculate r_{ch} from the matter radii r_m [1, 9, 20, 21, 22] we use $r_p = 0.862(12)$ fm, the neutron charge radius of the respective references, the standard Darwin-Foldy contribution, $r_{DF}^2 = 0.0331$ fm², the spin-orbit correction for the Paris potential $r_{SO}^2 = -0.0015$ fm², and the non-nucleonic contribution $r_{[2]}^2$ of column 3. In the last two rows the deuteron charge and matter radii are calculated from the experimental charge radius difference $(r_{ch}^2 - r_p^2)_{exp} = 3.795(19)$ fm² [14] and $(r_{ch}^2 - r_p^2)_{exp} = 3.807(26)$ fm² [23] as determined by the isotope shift of the $1s - 2s$ transition in atomic hydrogen. The value of Ref. [23] includes higher order QED effects. We calculate the corresponding deuteron matter and charge radii using the presently accepted values for the nucleonic radii, i.e., $r_p = 0.862(12)$ fm [17] and $r_n^2 = -0.113(3)$ fm² [18], $r_{DF}^2 = 0.0331$ fm², $r_{SO}^2 = -0.0015$ fm², and the two-nucleon contribution $r_{[2]}^2 = 0.0208$ fm² of this paper. The latter value is an average of our results for Δr_{MEC} for the Paris and the four Bonn potentials in Table 3.

$$r_d^2 = r_m^2 + r_{SO}^2 + r_{[2]}^2, \quad (6)$$

are summarized by two model-dependent corrections. We call these two corrections r_{SO}^2 and $r_{[2]}^2$.

The *first* one r_{SO}^2 is as r_{DF}^2 in Eq. (3) a relativistic correction which follows from the spin-orbit part of the one-nucleon charge operator, i.e.,

$$r_{SO}^2 = -6(2G_M^S(0) - G_E^S(0))P_D \frac{1}{8M_N^2}. \quad (7)$$

It is model-dependent, since it depends on the deuteron D -state probability P_D ; $2G_M^S(0) - G_E^S(0) = 0.76$, $G_M^S(\mathbf{Q}^2)$ being the isoscalar magnetic Sachs form factor of the nucleon. For example, for the D -state probability of the Paris potential, $P_D = 5.77\%$, one obtains $r_{SO}^2 = -0.0015 \text{ fm}^2$.

The *second* correction $r_{[2]}^2$ is formally defined by Eqs. (5) and (6). As difference between observable and unobservable quantities, $r_{[2]}^2$ is model-dependent. Conceptually, the term $r_{[2]}^2$ contains all contributions to the charge operator which are considered physically important and which are not accounted for by its single-nucleon parts. These corrections are usually of two-nucleon nature; this is the reason for the subscript [2]. Thus, $r_{[2]}^2$ has to contain two-nucleon meson-exchange corrections r_{MEC}^2 . It may contain relativistic boost corrections r_{boost}^2 not included by the standard use of nonrelativistic wave functions. It may contain Δ -isobar contributions $r_{\Delta\Delta}^2$ in interaction models with explicit Δ -isobar degrees of freedom which yield $\Delta\Delta$ -components in the deuteron wave function and corresponding charge and current operators. It may contain additional short-ranged quark-exchange effects r_{QEC}^2 . However, this list is not exhaustive given the ingenuity of theoreticians. We therefore write symbolically

$$r_{[2]}^2 = r_{MEC}^2 + r_{boost}^2 + r_{\Delta\Delta}^2 + r_{QEC}^2 + \dots \quad (8)$$

Nevertheless, as long as the model-dependent correction $r_{[2]}^2$ is small compared with the deuteron matter radius r_m , it makes sense to apply the corrections r_{SO}^2 and $r_{[2]}^2$ to data and extract that unobservable quantity r_m from them. The theoretical analyses of Table 2 usually combine data from several electron scattering experiments. They make the step from the structure radius r_d to an "experimental" matter radius r_m according to Eq. (6). However, most authors do not simply use Eq. (6), but reanalyse the original experimental data with some theoretical bias. The dependence of these analyses on P_D is only slight. The non-nucleonic correction $r_{[2]}^2$ is exclusively assumed to arise from one-pion exchange effects; the value $r_{[2]}^2 = r_{MEC}^2 = 0.0135 \text{ fm}^2$ due to calculations from Ref. [24] is often used. Compared with the single-experiment analyses of Table 1 we see that different theoretical analyses of elastic electron scattering data, usually based on several experiments, yield more consistent and with time even converging values. The deuteron matter radius r_m , the main result of those analyses, is listed in column 2 of Table 2; the resulting value of about 1.950 fm is in conflict, by 1%, with the value of 1.969 fm suggested by the experimental scattering length a_t according to the empirical linear relation. This discrepancy is considered serious. The analysis [25] of the Saclay data [13] is not included in Table 2. These data do not extend to sufficiently low \mathbf{Q}^2 to have by themselves a major impact on the deuteron radius. Nevertheless, Refs. [9, 25] conclude that the data set [13] favors a larger matter radius than the low-momentum transfer data sets.

In contrast to the theoretical analyses, we like to reconstruct values for the deuteron charge radius, listed in column 1. We obtain consistent values around 2.115 fm for it. However,

in the last two rows of Table 2 we also give our reinterpretation of the deuteron radius resulting from the atomic physics experiment [14] and from an analysis [23] of higher order QED corrections for it. Ref. [26] improves some of the corrections of Ref. [23]. A clear 1% discrepancy between the deuteron charge radius extracted from elastic electron scattering and from the atomic physics experiment surfaces and has been known for some time [10, 26]; this is a discrepancy between experimental data. This discrepancy remains unexplained and is disturbing. In addition and to the distress of theoreticians, no calculation based on realistic deuteron wave functions is able to account for the small deuteron charge radius as obtained from the elastic electron scattering experiments. This failure, being also of order 1%, has been demonstrated before for the deuteron matter radius r_m where the value resulting from the electron scattering data according to Table 2 ($r_m = 1.950(3)$ fm) and the value based on the experimental scattering length ($r_m = 1.969(4)$ fm) [1, 26], using the empirical linear relation of theoretical nature, are in serious conflict. The discrepancy between experimental data and theoretical predictions lead to the speculations of Refs. [3, 7, 8] that quark-gluon effects may show up in that observable.

The theoretical analyses, quoted in Table 2, require an assumption on the non-nucleonic correction $r_{[2]}^2$ of the deuteron radius which is model-dependent. Its meson-exchange correction has been calculated in the past in [24] for currents of pion-range only and in rather rough approximation. Though we expect corrections arising from heavier mesons to be rather unimportant, we conclude that a new determination of meson-exchange contributions to $r_{[2]}^2$ is necessary and timely. Furthermore, because of the recent speculations on exotic effects we also study the importance of quark-gluon corrections in $r_{[2]}^2$ using a nonrelativistic quark model of the deuteron. Both calculations are done in Sect. 3.

3. Theoretical Predictions for the Deuteron Charge Radius

The theoretical predictions are displayed in the form

$$r_{ch} = [r_m^2 + r_p^2 + r_n^2 + r_{DF}^2 + r_{SO}^2 + r_{[2]}^2]^{\frac{1}{2}}, \quad (9)$$

$$r_{ch} = [r_m^2 + r_p^2 + r_n^2]^{\frac{1}{2}} + \frac{r_{DF}^2 + r_{SO}^2 + r_{[2]}^2}{2[r_m^2 + r_p^2 + r_n^2]^{\frac{1}{2}}}, \quad (10)$$

$$r_{ch} = [r_m^2 + r_p^2 + r_n^2]^{\frac{1}{2}} + \Delta r_{DF} + \Delta r_{SO} + \Delta r_{[2]}. \quad (11)$$

Eq. (10) exploits the smallness of the corrections r_{DF}^2 , r_{SO}^2 and $r_{[2]}^2$; the equality holds better than 0.01% and this accuracy equals the computational accuracy. Eq. (11) defines the corrections Δr_{DF} , Δr_{SO} and $\Delta r_{[2]}$ in an obvious way; these corrections will be recorded in this paper. We prefer the linear form of the corrections, since the effect of contributions to the deuteron radius can be traced in a transparent way. However, the linear form also has a clear conceptual disadvantage: E.g., r_{DF}^2 is a model-independent number whereas $\Delta r_{DF} = r_{DF}^2/2[r_m^2 + r_p^2 + r_n^2]^{\frac{1}{2}}$ becomes model-dependent due to the denominator. Anyway, in the tables below, r_{DF}^2 , r_{SO}^2 and $r_{[2]}^2$ can always be recovered from the knowledge of $[r_m^2 + r_p^2 + r_n^2]^{\frac{1}{2}}$.

3.1. The Deuteron as a System of Hadrons

This subsection considers the deuteron as a system of hadrons. Only nucleon degrees of freedom are kept active, isobar and meson degrees of freedom are frozen into instantaneous potentials and instantaneous one- and two-nucleon currents. Nonrelativistic quantum mechanics is used; a relativistic boost correction is applied. Thus, the nontrivial correction $r_{[2]}^2$ is assumed to arise from meson exchange and relativistic boost corrections, i.e.,

	RSC	Paris	BonnQ	BonnA	BonnB	BonnC
π -pair	0.0050	0.0036	0.0043	0.0043	0.0047	0.0050
η -pair	-0.0001	-0.0001	-0.0001	-0.0001	-0.0001	-0.0000
ρ -pair	0.0001	0.0002	0.0005	0.0005	0.0003	0.0001
ω -pair	-0.0000	-0.0000	-0.0001	-0.0001	-0.0001	-0.0001
$\rho\pi\gamma$	0.0004	0.0003	0.0001	0.0001	0.0002	0.0002
π -ret	0.0002	0.0001	0.0001	0.0001	0.0001	0.0002
η -ret	0.0000	0.0000	0.0000	0.0000	0.0000	0.0000
ρ -ret	0.0000	0.0000	0.0001	0.0000	0.0000	0.0000
ω -ret	-0.0004	-0.0004	-0.0004	-0.0005	-0.0004	-0.0004
σ -ret	0.0005	0.0005	0.0005	0.0005	0.0005	0.0005
δ -ret	-0.0000	-0.0000	-0.0000	-0.0000	-0.0001	-0.0001
Δr_{MEC}	0.0057	0.0042	0.0050	0.0048	0.0051	0.0054

Table 3: **Meson-exchange contributions to the deuteron charge radius.** The individual contributions are given in fm for six two-nucleon potentials in the normalization Δr of Eq. (11); they are listed according to the exchange process (pair or ret as defined in Ref. [27]) and according to the exchanged meson. The row $\rho\pi\gamma$ corresponds to the only meson-nondiagonal process taken into account. The last row Δr_{MEC} contains the sum of all contributions. The last digit quoted in the entries is numerically unstable; however, trends reflected in the last digit appear correct.

$$r_{[2]}^2 = r_{MEC}^2 + r_{boost}^2. \quad (12)$$

The definition of meson-exchange currents is based on the extended S-matrix method of Ref. [27], and our use of it is described in Ref. [28]. Consistency of the meson-exchange currents with the underlying two-nucleon potential in form, i.e., with respect to the hadron form factors and with respect to the off-shell extrapolation parameters (μ, ν) , and in meson content is required. Calculations are carried out for six two-nucleon potentials, i.e., for the phenomenological Reid soft-core (RSC) [29], for the semiphenomenological Paris [30] and for four meson-exchange Bonn [31] potentials. The meson-exchange currents used correspond to all mesons which the Bonn potentials employ, i.e., the pseudoscalar mesons π and η , the vector mesons ρ and ω and the scalar mesons σ and δ . The required isoscalar charge operator is expanded in powers of (p/M_N) , p being a typical nucleon momentum in the nucleus, and its contributions up to the relativistic order $(p/M_N)^2$ are retained. The physics content of the meson-diagonal contributions contact/pair (pair) and retardation (ret) is explained in Ref. [27]; among the meson-nondiagonal contributions only the $\rho\pi\gamma$ part is kept. In this paper, we have not calculated the effect of *explicit* $\Delta\Delta$ wave function components [32] on the deuteron charge radius. Taking $\Delta\Delta$ components explicitly into account, Ref. [2] sees an increase of the deuteron matter radius, Ref. [33], however, a decrease due to subsequent meson-exchange corrections; a further study of that cancellation is indicated.

Our results are collected in Tables 3 and 4. The break-down of the meson-exchange correction Δr_{MEC} into individual contributions is given in Table 3. Their potential dependence is moderate, at most 20%. The dominant contribution arises from the π -contact term in pseudovector πNN coupling, which is equivalent to the pair term in pseudoscalar coupling. Previous calculations often used contributions of pion range only. The result mostly used is that of Ref. [24] which is based on the Paris potential. We agree with that result within

	RSC	Paris	BonnQ	BonnA	BonnB	BonnC
r_m	1.9569	1.9717	1.9684	1.9692	1.9689	1.9675
$\sqrt{r_m^2 + r_p^2 + r_n^2}$	2.1118	2.1255	2.1224	2.1232	2.1229	2.1216
Δr_{DF}	0.0078	0.0078	0.0078	0.0078	0.0078	0.0078
Δr_{SO}	-0.0004	-0.0003	-0.0003	-0.0003	-0.0003	-0.0003
Δr_{MEC}	0.0057	0.0042	0.0050	0.0048	0.0051	0.0054
r_{ch}	2.1249	2.1372	2.1349	2.1355	2.1355	2.1345

Table 4: **Contributions to the charge radius in the hadronic description of the deuteron.** The contributions are given in fm for six two-nucleon potentials in the normalization Δr of Eq. (11). The boost correction Δr_{boost} is kinematical in the case of the deuteron; it is also calculated, but turns out to be zero for all retained digits. Thus, the non-nucleonic correction $\Delta r_{[2]}$ is identical to Δr_{MEC} given in Table 3, i.e., $\Delta r_{[2]} = \Delta r_{MEC}$.

10%, but our inclusion of more processes and more mesons makes Δr_{MEC} larger by about 15%.

The results for the deuteron charge radius are given in Table 4. We consider the result derived from the RSC potential unreliable mainly because the RSC triplet scattering length is unrealistically small. In addition, the construction of a consistent MEC operator for a phenomenological potential such as the RSC potential would require some extra effort [34]. Nevertheless, we list the results of the old-fashioned RSC potential as reference for the computational comparison with previous calculations. The results for the other potentials show a small spread only; they cluster around the value 2.135 fm. They favor the value obtained in the atomic physics experiment as Ref. [26] also concludes for its calculations. According to the results of Refs. [2, 33] this conclusion will remain firm even if effects of $\Delta\Delta$ -components in the deuteron wave function were taken into account.

3.2. The Deuteron as a Six-Quark System

This section considers the deuteron as a system of six nonrelativistic quarks. The six-quark deuteron wave function is fully antisymmetrized; it is obtained according to the *Resonating Group Method* (RGM); only the channel with two asymptotic nucleons is retained. However, even a single channel calculation leads to a deuteron wave function which has $\Delta\Delta$ and hidden color admixtures in the short-range region [35]. This is a consequence of the Pauli principle at the quark level.

The calculation is based on a chiral-invariant quark hamiltonian with instantaneous two-quark potentials; the interaction contains a quadratic confinement potential and residual interactions due to gluon-, π - and σ -exchange.

Fig. 2 displays the quark-quark interaction; the antisymmetrizer for the six-quark wave function is considered as part of the displayed interaction operator. The antisymmetrizer acts on the product wave function of two three-quark clusters with nucleon quantum numbers correlated by a relative cluster-cluster wave function which is not yet antisymmetrized with respect to quarks belonging to different clusters.

Two models are investigated for the deuteron. In the first one, called model A, the quark hamiltonian is taken into account in full within the RGM calculation of Ref. [37]. Compared with the traditional purely nucleonic two-nucleon potentials, model A yields an *attractive* nonlocal effective two-nucleon interaction at small relative distances which arises from σ -exchange with simultaneous quark interchange shown in Figs. 2(b-c) and 2(e-g). The

second one, called model B, simplifies the dynamics by retaining only the *direct* σ -exchange between three-quark nucleon clusters shown in Fig. 2(d). In model B the intracuster σ -exchange diagram of Fig. 2(a) and the σ -exchange diagrams with simultaneous quark interchange of Figs. 2(b-c) and 2(e-g) are omitted; the attraction at small relative distances is less pronounced compared with model A.

The comparison of the results of models A and B shows the importance of the attractive nonlocality due to the σ -quark exchange diagrams of Figs. 2(b-c) and 2(e-g) for the deuteron charge radius. Due to the attractive nonlocality at small distances, the deuteron wave function of model A, i.e., the relative wave function between nucleonic three-quark clusters, properly renormalized to account for the norm kernel according to Ref. [36], shows an increased probability at small relative distances with respect to model B. Compared with the purely nucleonic Paris potential wave function, both wave functions of model A and B have a slightly increased probability at small internucleon distances but are otherwise similar to that of the Paris potential. The six-quark deuteron wave function does not exhibit any exotic structures at small relative distances in contrast to the speculations of Refs. [7, 8].

The charge and current of the deuteron is carried by the quarks. Sample processes for the charge operators are displayed in Fig. 3. In addition to the single-quark charge operator of Figs. 3(a-c) there are exchange corrections of two-quark nature; they arise from gluon-, π - and σ -exchange according to Figs. 3(d-j). Only gluon- and π -exchange currents are considered in the calculation. Currents arising from σ -exchange are not taken into account; they are assumed to be smaller than those of pion range according to the general experience with σ -meson exchange currents between hadrons. The quark processes of Fig. 3 can be resummed (i) into those of single-nucleon character, (ii) into those of two-nucleon π -exchange character, and (iii) into novel ones of quark-exchange character, called quark-exchange currents (QEC). Especially, the relative weight of these three processes is important for the discussion of this paper. The quark-exchange current is defined as the sum of all processes calculated with the proper six-quark wave functions minus the processes (a), (d) and (g) calculated with renormalized wave functions. In other words, the difference between processes (a), (d) and (g) calculated with unrenormalized and renormalized six-quark wave functions has to be added to the contributions of diagrams (b), (c), (f), (h-j) in order to obtain the proper quark exchange current [36]. A more detailed discussion of the charge and current model is given in Ref. [36].

Our results are given in Tables 5 and 6. Table 5 gives a break-down of the quark-exchange processes into individual contributions. Table 6 sums the results up to the charge radius. The difference in the predictions for models A and B shows that the short-ranged nonlocal attraction due to Figs. 2(b-c) and 2(e-g) indeed leads to some redistribution of matter towards shorter distances which affects already the deuteron matter radius and therefore the impulse approximation to the charge radius. We find that the novel quark-exchange current contributions to the deuteron charge radius amount to about 20% of the traditional π -meson exchange contribution; they are therefore of the same size as the non-pionic exchange current corrections considered in Subsect. 3.1. The e.m. QEC corrections are, however, smaller than the quark exchange effects generating the attractive nonlocality responsible for the redistribution of matter to smaller distances.

With respect to the speculations that quark-gluon effects may be important for the theoretical prediction of the deuteron charge radius, we therefore have to conclude that our calculations do not support them. As expected, the hadronic description of the deuteron together with the meson-exchange corrections of Subsect. 3.1 remains valid. Furthermore, the discrepancy between the deuteron charge radius as extracted from elastic electron scattering data and its theoretical prediction remains also in a quark model description of the

	Model A	Model B
impulse	0.0001	0.0001
π -pair	0.0003	0.0004
gluon	0.0004	0.0004
Δr_{QEC}	0.0008	0.0009

Table 5: **Quark-exchange contributions to the deuteron charge radius.** The contributions are given in fm for the two quark models A and B in the normalization Δr of Eq. (11). Row 1: impulse charge operator with quark exchange according to Figs. 3(b-c). Row 2: pion-pair charge operator with quark exchange according to Figs. 3(e-f), 3(h-j). Row 3: gluon-pair charge operator with quark exchange according to Figs. 3(e-f), 3(h-j). The last row Δr_{QEC} contains the sum of all contributions. The last digit quoted in the entries is numerically unstable; however, trends reflected in the last digit appear correct.

	Model A	Model B
r_m	1.9657	1.9680
$\sqrt{r_m^2 + r_p^2 + r_n^2}$	2.1199	2.1220
Δr_{DF}	0.0078	0.0078
Δr_{SO}	-0.0004	- 0.0004
Δr_{MEC}	0.0043	0.0044
Δr_{QEC}	0.0008	0.0009
r_{ch}	2.1324	2.1348

Table 6: **Contributions to the charge radius in the six-quark description of the deuteron.** The contributions are given in fm for the two models A and B in the normalization Δr of Eq. (11); they are graphically displayed in Fig. 3. The processes of Figs. 3(a) and 3(d) correspond to the conventional ones of a single-nucleon charge operator; the results are given in the first four rows; the experimental values $r_p = 0.862(12)$ fm [17] and $r_n^2 = -0.113(3)$ fm [18] are used. With the small quark core radius $b = 0.5184$ fm used here the experimental proton and neutron charge radii are not exactly reproduced by the underlying quark model; see however [38]. The meson-exchange correction Δr_{MEC} accounts for the process of Fig. 3(g); it corresponds to the canonical pion-pair term in the hadronic description of the deuteron. The processes of Figs. 3(b-c), 3(e-f), 3(h-j) have no counterpart in the hadronic description; they yield the novel quark exchange contributions Δr_{QEC} ; their individual contributions are listed in Table 5.

deuteron.

4. Conclusion

We recall: For a long time the electron scattering data of Ref. [12], yielding a deuteron charge radius of about 2.115 fm, were considered valid beyond any reasonable doubt. In fact, the value for the proton charge radius [17], still unquestioned as standard, is derived from the same experiment. Thus, the inability of the purely nucleonic deuteron description to account for a deuteron charge radius of 2.115 fm – the theoretical predictions clustering around 2.135 fm are off by 1% – was taken to be a pure *theory problem*. Speculations on exotic effects surfacing in the deuteron charge radius started to flourish, though the deuteron size is dominated by the wave function tail, the regime in which the two nucleons are well separated. The appearance of the electron scattering data of Ref. [13] changed that situation. In principle, the experiment of Ref. [13] cannot provide very detailed information on the deuteron charge radius; it measures the structure function $A(\mathbf{Q}^2)$ at intermediate momentum transfers, but there it is in disagreement with Ref. [12]; thus, the suspicion arose that the discrepancy between experimental value and theoretical prediction may be rooted in an *experimental problem* after all. This suspicion gets now further support by the result of the atomic physics experiment [14] which suggests a larger experimental deuteron charge radius of 2.130 fm consistent with the theoretical value. When making this conclusion we assume that e.m. corrections beyond one-photon exchange are – on the level of a 1% comparison – the same for a bound and a scattered electron; in fact, this holds true in case of the proton for which electron scattering and an atomic physics experiment [39] yield consistent data. The recalled historic evolution of the problem provides the background for the present paper.

This paper presents a recalculation of the deuteron charge radius within a purely nucleonic picture of the nucleus, with a complete set of meson-exchange corrections included in the charge operator. A corresponding calculation within a six-quark picture of the deuteron yields only a tiny additional correction of the order of 0.1% arising from processes of true quark nature, which are not accounted for in the hadronic description. The size of this quark correction is consistent with a previous rough estimate [8]. As expected, the hadronic description of the deuteron radius is valid. Quark-gluon effects are very small for the static charge properties of a nuclear system bound as lightly as the deuteron.

Our theoretical predictions are based on six realistic two-nucleon potentials and on a nonrelativistic constituent quark model. All yield a value of about 2.135 fm for the deuteron charge radius. Only the value for RSC is, with 2.125 fm, significantly smaller; we mistrust the RSC value at this level of precision for the reasons discussed in sect. 3.1. Our theoretical predictions of about 2.135 fm disagree with the experimental values of around 2.115 fm obtained in the analyses of elastic electron scattering data and quoted in Table 2. We therefore also present our predictions for the deuteron longitudinal structure function $A(\mathbf{Q}^2)$ at finite momentum transfers \mathbf{Q} in Fig. 4 which shows how the two principal data sets [12] and [13] are in conflict. This conflict suggests that a remeasurement of $A(\mathbf{Q}^2)$ in elastic electron scattering, especially at low momentum transfers, is necessary. According to Fig. 4, our predictions can describe the data set of Ref. [13] which, however, has only little impact on the deuteron charge radius, and therefore was left out from Table 2. Nevertheless, the data of Ref. [13] have a trend that favors a larger charge radius consistent with the atomic physics experiment as was already noticed in Ref. [9, 25]. This conclusion is derived from the observation that all theoretical predictions for $A(\mathbf{Q}^2)$ in the intermediate momentum transfer range of Fig. 4 are ordered according to their values for the charge radius: Experimentally, data in the intermediate momentum transfer regime provide no information on the charge radius; theoretically, however, the underlying hadronic force and current model

seems to provide a rather rigid relation between the e.m. properties at low and intermediate momentum transfers.

Finally, we note that the theoretical prediction of this paper for r_{ch} which includes a complete set of exchange current operators and quark-gluon corrections is in agreement with the deuteron charge radius obtained in the recent atomic physics measurement [14, 23].

Added Note

After submitting this paper, a reanalysis of the relevant data on elastic electron-deuteron scattering including two-photon exchange corrections appeared [40]. The newly extracted deuteron charge radius $r_{ch} = 2.128(11)$ fm [40] is consistent with the atomic physics experiment and theoretical predictions.

Acknowledgement

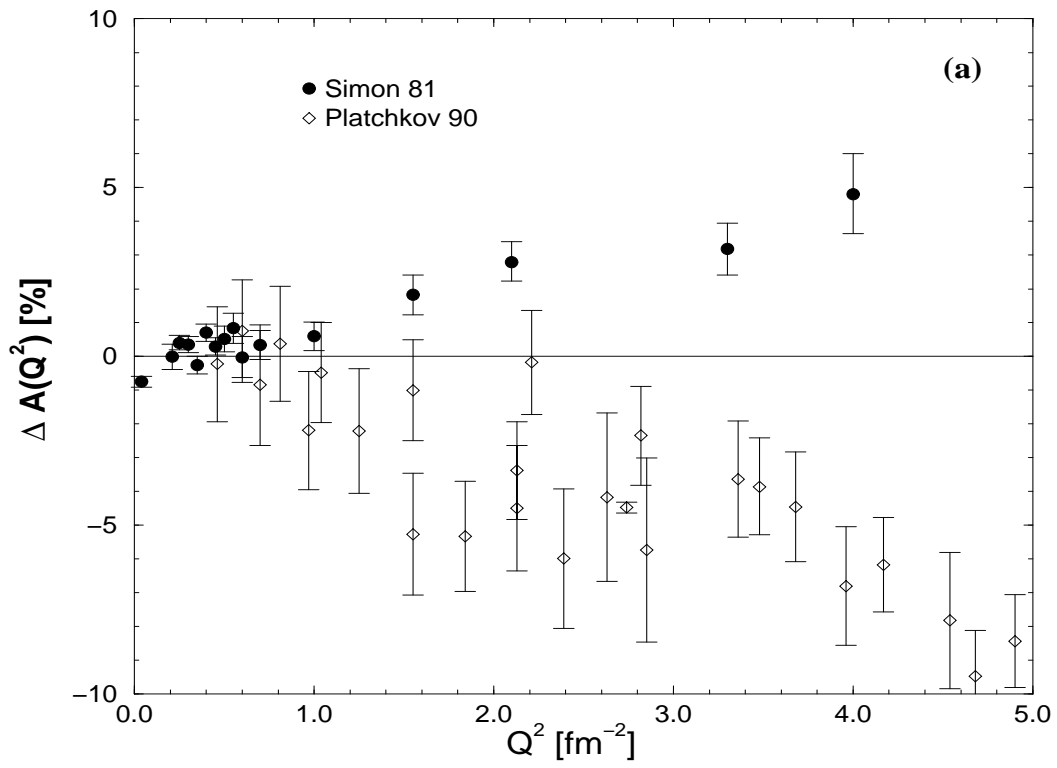
The authors gratefully acknowledge helpful discussions with I. Sick and D. W. L. Sprung. The calculations were done at Regionales Rechenzentrum für Niedersachsen (RRZN), Hannover.

References

- [1] S. K. Klarsfeld, J. Martorell, J. A. Oteo, M. Nishimura and D. W. L. Sprung, Nucl. Phys. **A456** (1986) 373
- [2] R. K. Bhaduri, W. Leidemann, G. Orlandini and E. L. Tomusiak, Phys. Rev. **C42** (1990) 147
- [3] D. W. L. Sprung, Hua Wu and J. Martorell, Phys. Rev. **C42** (1990) 863
- [4] M. W. Kermode, S. A. Moszkowski, M. M. Mustafa and W. van Dijk, Phys. Rev. **C43** (1991) 416
- [5] W. van Dijk, Phys. Rev. **C40** (1989) 1437
- [6] G. M. Shklyarevsky, J. Phys. **G20** (1994) 1035
- [7] M. W. Kermode, W. van Dijk, D. W. L. Sprung, M. M. Mustafa, and S. A. Moszkowski, J. Phys. **G17** (1990) 105
- [8] C. W. Wong, Phys. Lett. **B291** (1992) 363
- [9] C. W. Wong, Int. J. Mod. Phys. **E3** (1994) 821
- [10] P. U. Sauer and H. Henning, Few-Body Systems, Suppl. **7** (1994) 92
- [11] R. G. Arnold, C. Carlson and F. Gross, Phys. Rev. **C42** (1980) 863
- [12] G. G. Simon, Ch. Schmitt and V. H. Walther, Nucl. Phys. **A364** (1981) 285
- [13] S. Platchkov *et al.*, Nucl. Phys. **A510** (1990) 740
- [14] F. Schmidt-Kaler, D. Leibfried, M. Weitz and T. W. Hänsch, Phys. Rev. Lett. **70** (1993) 2261
- [15] R. W. Berard, F. R. Buskirk, E. B. Dally, J. N. Dyer, X. K. Maruyama, R. L. Topping and T. J. Traverso, Phys. Lett. **B47** (1973) 355

- [16] Yu. K. Akimov *et al.*, Sov. J. Nucl. Phys. **29** (1979) 335
- [17] G. G. Simon, Ch. Schmitt, F. Borkowski and V. H. Walther, Nucl. Phys. **A333** (1980) 381
- [18] S. Kopecky, P. Riehs, J. A. Harvey and N. W. Hill, Phys. Rev. Lett. **74** (1995) 2427
- [19] V. G. J. Stoks, P. C. van Campen, W. Spit, and J. J. de Swart, Phys. Rev. Lett. **60** (1988) 1932;
I. Borbely *et al.*, Phys. Lett. **B160** (1985) 17;
M. W. Kermode, A. McKerrell, J. P. McTavish, and L. J. Allen, Z. Phys. **A303** (1981) 167
- [20] L. J. Allen, J. P. McTavish, M. W. Kermode and A. McKerrell, J. Phys. **G7** (1981) 1367
- [21] J. P. McTavish, J. Phys. **G8** (1982) 911
- [22] M. M. Mustafa, Phys. Rev. **C48** (1993) 929
- [23] K. Pachucki, M. Weitz and T. W. Hänsch, Phys. Rev. **C49** (1994) 2255
- [24] M. Kohno, J. Phys. **G9** (1983) L85
- [25] D. W. L. Sprung and Hua Wu, Acta Phys. Pol. **B24** (1993) 503
- [26] J. Martorell, D. W. L. Sprung and D. C. Zheng, Phys. Rev. **C51** (1995) 1127
- [27] J. Adam Jr., E. Truhlik and D. Adamova, Nucl. Phys. **A492** (1989) 556
- [28] H. Henning, J. Adam and P. U. Sauer, Few-Body Systems, Suppl. **5** (1992) 133;
H. Henning, J. Adam, P. U. Sauer and A. Stadler, Phys. Rev. **C52** (1995) R471
- [29] R. V. Reid, Ann. of Phys. **50** (1968) 411
- [30] M. Lacombe, B. Loiseau, J. M. Richard, R. Vinh Mau, J. Cote, P. Pires and R. de Tourreil, Phys. Rev. **C21** (1980) 861
- [31] R. Machleidt, K. Holinde and Ch. Elster, Phys. Rep. **149** (1987) 1;
R. Machleidt, Adv. Nucl. Phys. **19** (1989) 189
- [32] P. Obersteiner, W. Plessas and J. Pauschenwein, Few-Body Systems, Suppl. **5** (1992) 140
- [33] M. G. Vassanji, F. C. Khanna and I. S. Towner, J. Phys. **G7** (1981) 1029
- [34] A. Buchmann, W. Leidemann and H. Arenhövel, Nucl. Phys. **A443** (1985) 726;
D. O. Riska, Phys. Scripta **31** (1985) 471
- [35] Amand Faessler, F. Fernandez, G. Luebeck and K. Shimizu, Nucl. Phys. **A402** (1983) 555
- [36] A. Buchmann, Y. Yamauchi and Amand Faessler, Nucl. Phys. **A496** (1989) 621;
A. Buchmann, Y. Yamauchi, Hiroshi Ito and Amand Faessler, J. Phys. **G14** (1988) 1037

- [37] A. Valcarce, A. Buchmann, F. Fernandez and A. Faessler Phys. Rev. **C50** (1994) 2246
- [38] A. Buchmann, E. Hernandez and K. Yazaki, Phys. Lett. **B269** (1991) 35; Nucl. Phys. **A569** (1994) 661
- [39] M. Weitz, F. Schmidt-Kaler and T. W. Hänsch, Phys. Rev. Lett. **68** (1992) 1120
M. Weitz, A. Huber, F. Schmidt-Kaler, D. Leibfried and T. W. Hänsch, Phys. Rev. Lett. **72** (1994) 328
Krzysztof Pachucki, Phys. Rev. Lett. **72** (1994) 3154
- [40] I. Sick and D. Trautmann, Phys. Lett. **B375** (1996) 16



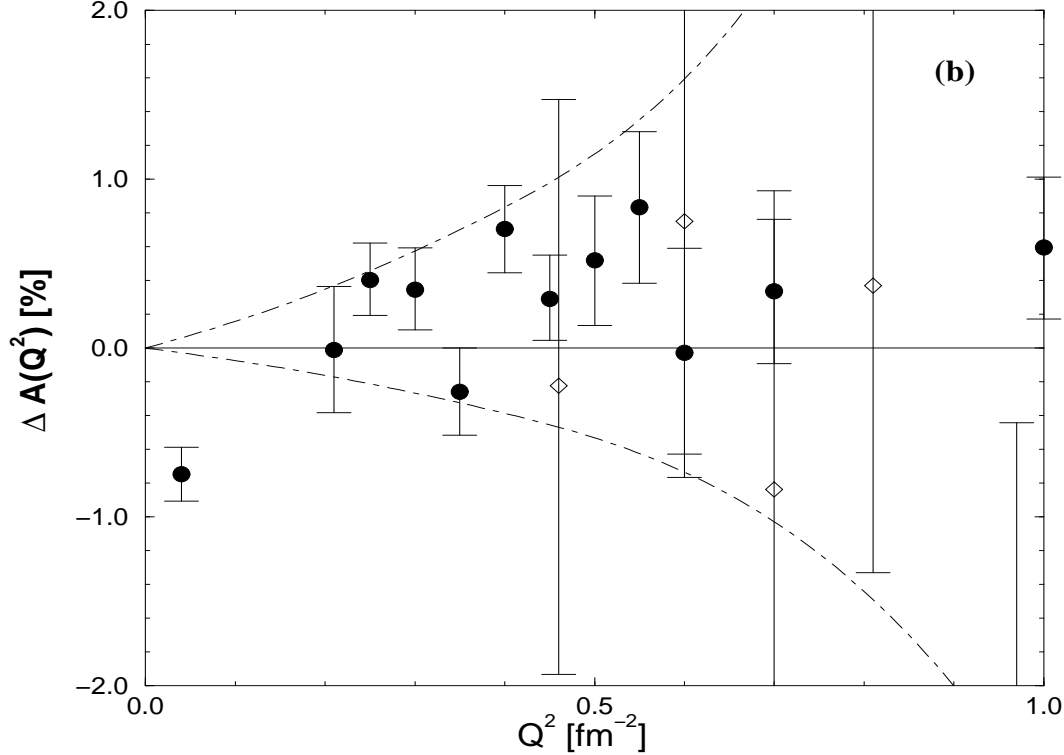


Figure 1: **(a)** Experimental data for the longitudinal deuteron structure function $A(\mathbf{Q}^2)$. A high-resolution representation $\Delta A(\mathbf{Q}^2) = (A(\mathbf{Q}^2) - A_{IA,Paris}(\mathbf{Q}^2))/A_{IA,Paris}(\mathbf{Q}^2) * 100$ is chosen. $A_{IA,Paris}(\mathbf{Q}^2)$ is the theoretical result derived from the Paris potential in nonrelativistic impulse approximation using the nucleonic Dirac form factor $F_1^S(\mathbf{Q}^2)$ instead of the Sachs form factor $G_E^S(\mathbf{Q}^2)$ in the nonrelativistic charge operator. The data are plotted in the Breit frame as a function of $\mathbf{Q}^2 = -q^2$, q being the four-momentum transfer. The two elastic electron scattering data sets of Refs. [12] (bullets) and [13] (diamonds) appear to be inconsistent; for this conclusion data up to $\mathbf{Q}^2 = 5 \text{ fm}^{-2}$ are shown.

(b) An attempt is made to indicate the importance of the deuteron charge radius for the determination of the structure function $A(\mathbf{Q}^2)$ at small momentum transfers. The lower dashed-dotted curve refers to the linear approximation $A(\mathbf{Q}^2) = (1 - r_{ch}^2 \mathbf{Q}^2/6)^2$ with $r_{ch} = 2.1303 \text{ fm}$ from the atomic physics experiment [14]. The upper dashed-dotted curve shows the corresponding linear approximation for the charge radius $r_{ch} = 2.1146 \text{ fm}$ resulting from the analysis [1] of the elastic electron scattering experiments [12] and [15]. The reference result $A_{IA,Paris}(\mathbf{Q}^2)$ is linearized in the same way for these theoretical curves. We note that the charge radius 2.1303 fm of Ref. [14] is inconsistent with the low momentum transfer data of Ref. [12], but seems to be consistent with the Saclay data. In the context of Fig. 4 we shall note that the linear approximation is poor at momentum transfers \mathbf{Q}^2 larger than 0.5 fm^{-2} . Thus, the extrapolation of the elastic electron scattering data to the slope of $A(\mathbf{Q}^2)$ or $F_{ch}(\mathbf{Q}^2)$ at zero momentum transfer has to be done with great care.

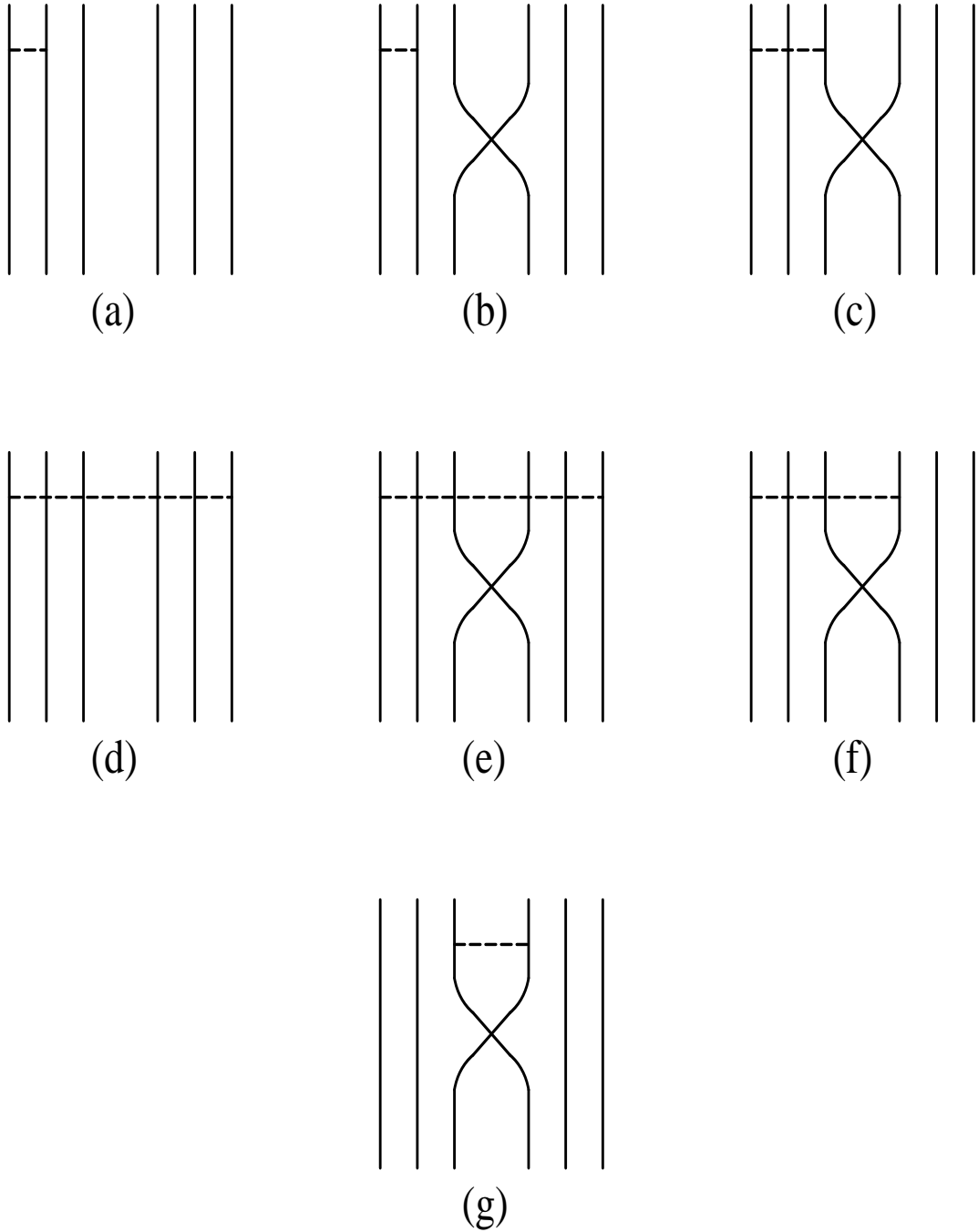


Figure 2: Sample contributions to the two-nucleon interaction arising from meson-exchange in a quark model description of the deuteron. The horizontal dashed line stands for the meson; σ -exchange is chosen here as an example. Process (a) is the intracluster term, process (d) the direct intercluster term and the other processes are quark-exchange terms. The quark model A includes all σ -exchange processes, quark model B only the intercluster σ -exchange process (d) without quark exchange terms. In contrast to Ref. [36] both models A and B employ σ -exchange between quarks and not between the centers of three-quark clusters.

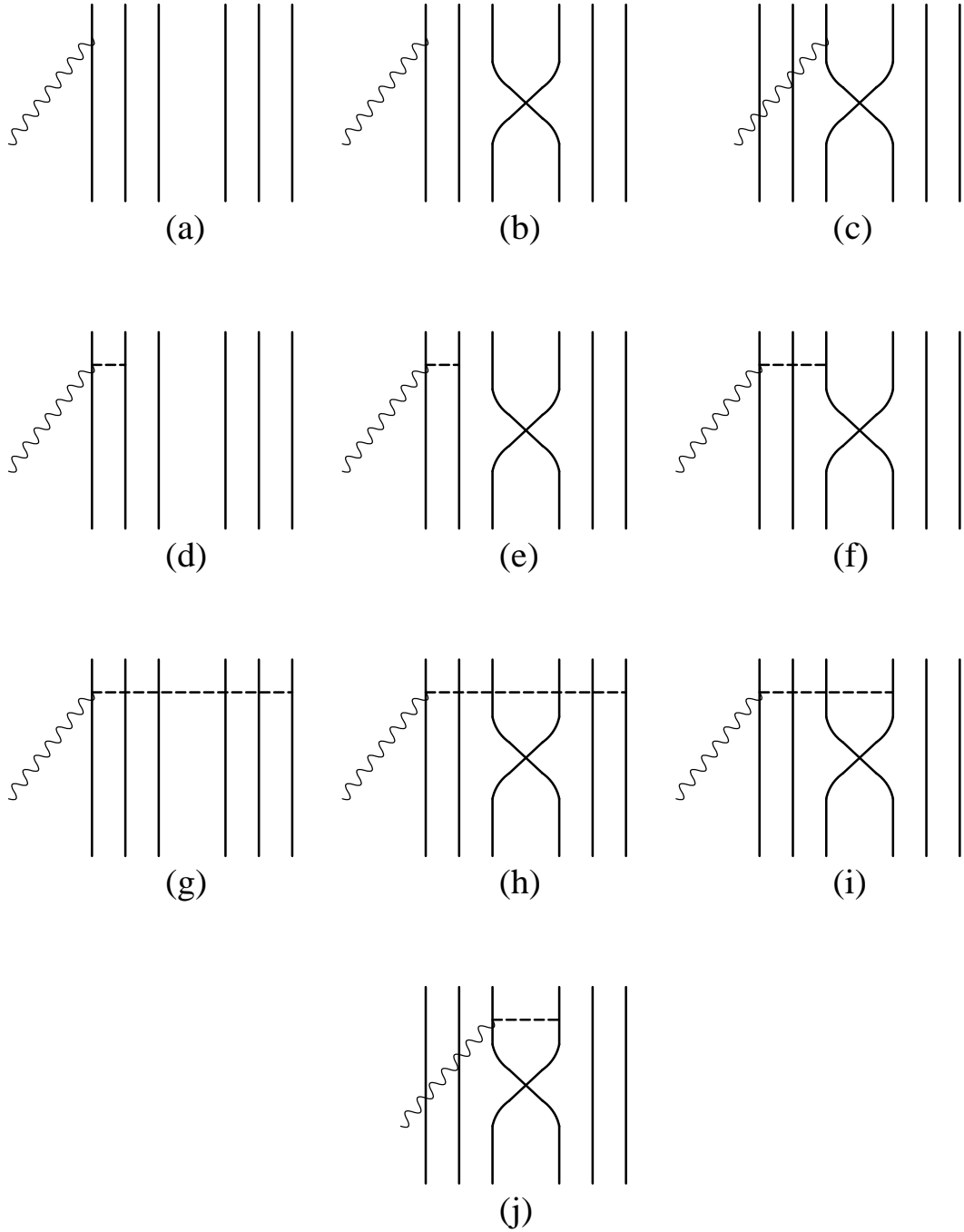


Figure 3: Sample contributions to the one-nucleon and two-nucleon currents in a quark description of the deuteron. The current has single-quark and irreducible two-quark parts. The single-quark current can be split into direct and quark-exchange pieces according to processes (a) and (b), (c), respectively. The two-quark current arises from π - and gluon-exchange; only the π -exchange is indicated as horizontal dashed line in the figure. The two-quark current can be split into direct intracluster (d), direct intercluster (g) and the quark-exchange processes (e), (f), (h)-(j). Processes (a) and (d) correspond to the single-nucleon current and process (g) to the two-nucleon pion-exchange current in a hadronic description when calculated with renormalized six-quark wave functions. The break-down of the quark-exchange processes into quark-exchange impulse, quark-exchange pion and quark-exchange gluon given in Table 5 is now obvious.

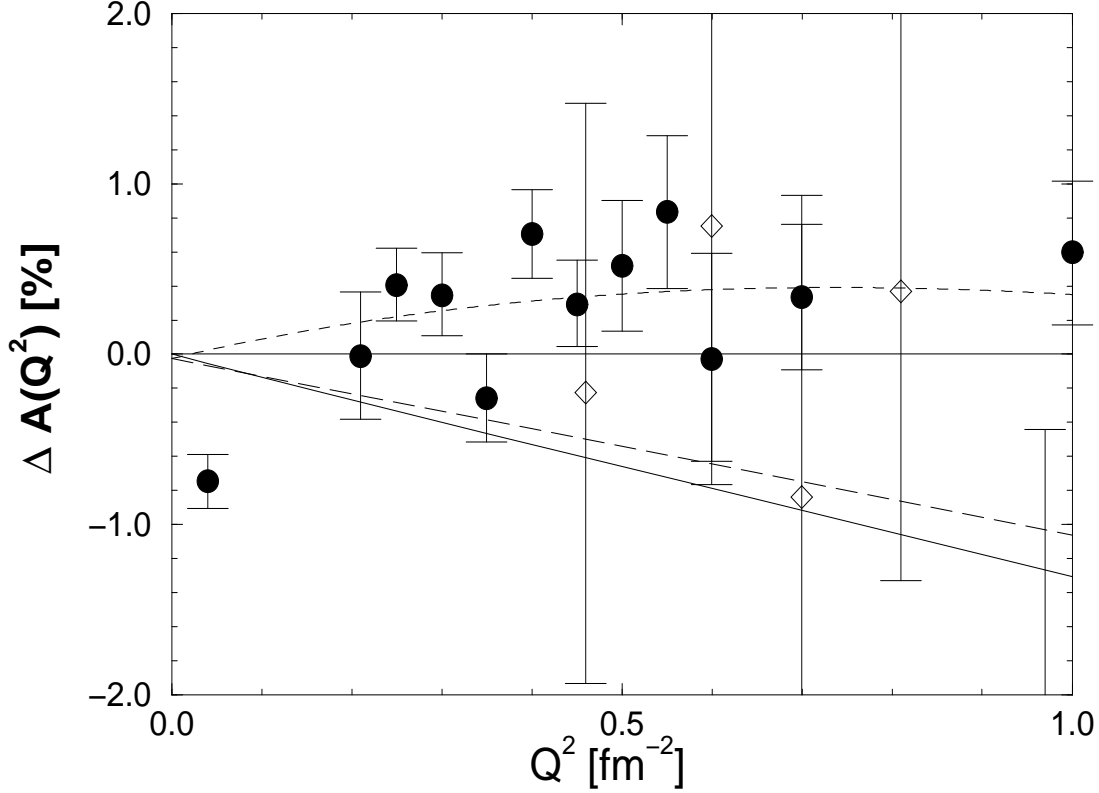


Figure 4: Longitudinal deuteron structure function $A(Q^2)$. A high resolution representation $\Delta A(Q^2) = (A(Q^2) - A_{IA,Paris}(Q^2))/A_{IA,Paris}(Q^2) * 100$ is chosen. $A_{IA,Paris}(Q^2)$ is the theoretical result derived from the Paris potential in nonrelativistic impulse approximation using the nucleonic Dirac form factor $F_1^S(Q^2)$ instead of the Sachs form factor $G_E^S(Q^2)$ for the nonrelativistic charge operator. Theoretical predictions for three realistic two-nucleon potentials RSC, Paris and Bonn C, shown as dotted, solid, and dashed curves, respectively, are compared with the data. The results for the Bonn A and B potentials cluster around the Bonn C curve; our prediction for the charge radius of the Bonn C potential, $r_{ch} = 2.1345$ fm (see table 4) is consistent with the atomic physics experiment (table 2). We note that the linear approximation for $\Delta A(Q^2)$, used in Fig. 1 to emphasize the different trend for $\Delta A(Q^2)$ arising from different charge radii, is not valid anymore for momentum transfers Q^2 larger than 0.5 fm^{-2} . We observe that the theoretical predictions for the Paris and for all Bonn potentials cannot explain the data of Ref. [12]; however, they appear to be consistent with the data set of Ref. [13].